Turkish Journal of Electrical Engineering & Computer Sciences

http://journals.tubitak.gov.tr/elektrik/

Research Article

Turk J Elec Eng & Comp Sci
(2017) 25: 4696 – 4705

doi:10.3906/elk-1704-209

A novel approach to solve transient stability constrained optimal power flow problems

Huy NGUYEN-DUC[1,*], Linh TRAN-HOAI[1], Dieu VO NGOC[2]
[1]School of Electrical Engineering, Hanoi University of Science and Technology, Hanoi, Vietnam
[2]Department of Power Systems, Ho Chi Minh City University of Technology, Ho Chi Minh City, Vietnam

Received: 18.04.2017 • **Accepted/Published Online:** 15.09.2017 • **Final Version:** 03.12.2017

Abstract: This paper proposes an approach to solve the transient stability constraint optimal power flow (TSC-OPF) problem. The transient stability constraints are expressed as the critical clearing time (CCT) of different contingencies, and are approximated using artificial neural networks (ANNs). The ANNs provide a nonlinear, differentiable mapping between the load flow variables and the CCT. As a result, the TSC-OPF with multiple transient stability constraints can be solved very efficiently with little additional computational burden. The effectiveness of the proposed method is demonstrated with the IEEE 39 bus and the IEEE 300 bus systems.

Key words: Power system stability, critical clearing time, transient stability constrained optimal power flow, artificial neural networks

1. Introduction

During the real-time operation and planning of electric power systems, having a rapid and accurate assessment of the power system stability boundary is an essential requirement. According to the definition and classification of IEEE/CIGRE [1], power system stability can be divided into 3 categories: frequency, voltage, and rotor angle stability. The large disturbance rotor angle stability, which is often referred to as transient stability, is the ability of the power system generators to remain in synchronism after severe short-circuit faults. An accurate assessment of transient stability requires a detailed time domain simulation, which is a computationally extensive study, particularly when several contingencies must be considered.

A stability-constrained optimal power flow is essentially a traditional OPF formulation coupled with additional constraints to consider various stability constraints [2–5]. A common solution to include transient stability constraints into an OPF problem is to use discretized dynamic equations as the constraints. The main disadvantage of this approach is that the number of constraints of the transient stability-constrained optimal power flow (TSC-OPF) problem is very large, which significantly increases the computation burden.

Recently, many studies have proposed using independent dynamic simulation in the TSC-OPF framework. References [6–8] propose the use of an independent dynamic simulation code to determine the transient stability at each iteration step. The drawback to this approach is that there is no explicit analytical expression between the transient stability boundary and the optimization variables, which enables the gradient of the stability boundary to be derived, with regard to the optimization variables. Without the gradient information, the convergence rate would be slow.

*Correspondence: huy.nguyenduc1@hust.edu.vn

To improve the convergence rate of TSC-OPF algorithms, several studies have proposed the use of sensitivity analysis. The results of [9–11] clearly show that sensitivity-based algorithms can help reduce the computation time of the TSC-OPF problem. However, time-domain simulations remain necessary during the OPF calculation. The computation time for contingency simulation can be substantial, particularly when several contingencies are considered.

In addition to the conventional gradient-based method, several studies also proposed heuristic algorithms to solve the TSC-OPF problem [12–17]. However, heuristic algorithms usually incur very high computational cost. Reference [18] proposed a multiobjective genetic algorithm, based on the Pareto front principle. This approach can potentially reduce the computation time, because the optimization is stopped when there is no further improvement in the CCT and the overall objective function.

This paper proposes an alternative approach to solve the TSC-OPF problem, where the transient stability constraints are approximated using artificial neural networks (ANNs). The study is motivated by previous research, which showed that the CCT can be approximated with very high accuracy from prefault load flow data using various artificial intelligence networks [19–22]. Hence, the ANNs can provide analytical expressions of the stability boundaries and their sensitivity with respect to optimization variables.

The paper is organized as follows: Section 2 introduces some background on the problem of OPF with augmented stability constraints, and Sections 3 and 4 present the proposed approach of using ANNs to approximate the system's CCT. Section 5 presents the results obtained with the New England 39 bus system and the IEEE 300 bus system.

2. TSC-OPF

The TSC-OPF problem is an extended formulation of the conventional OPF. The original OPF problem consists of minimizing an objective function by generation scheduling, as follows:

$$f\left(P_g\right) \rightarrow min \tag{1}$$

The steady-state constraints are essentially power flow equations at system buses and their physical limits:

$$P_g - P_L - P\left(U,\theta\right) = 0 \tag{2}$$

$$Q_g - Q_L - Q\left(U,\theta\right) = 0 \tag{3}$$

$$U_{\min} \leq U \leq U_{\max} \tag{4}$$

$$P_{g.\min} \leq P_g \leq P_{g.\max} \tag{5}$$

$$Q_{g.\min} \leq Q_g \leq Q_{g.\max} \tag{6}$$

In Eqs. (2)–(6), P_g and P_L are the active injected power and the active load at the system buses, respectively. Similarly, Q_g and Q_L are the reactive power injected and the reactive load at system buses. The functions $P\left(U,\theta\right)$ and $Q\left(U,\theta\right)$ are the power flow equations, and U is the vector of bus voltages, where $U_{\min}$ and $U_{\max}$ are the lower and upper limits. The generators active and reactive power are also subjected to operating constraints, as shown in Eqs. (5) and (6).

The TSC-OPF problem extends the OPF formulation by adding constraints that are related to the stability criteria. In the most direct form, these constraints can be written as

$$CCT_k\left(P_g, Q_g, U, \theta\right) \geq CCT_{\min},\ k = 1, .., N, \tag{7}$$

where subscript k denotes the kth contingency. However, there is no analytical function for CCT as in Eq. (7) because time-domain simulations must be performed to determine the CCT values. As discussed in Section 1, in order to derive an approximate analytical expression of Eq. (7), several research works proposed a sequential approach, where the stability boundary is estimated outside the OPF calculation [7,9,16–18]. However, because there is no analytical function of the stability margin, the convergence rate of the optimization can be slower than that of a conventional OPF. In addition, the time required at each optimization step to determine the CCT is considerable. To increase the convergence rate, CCT sensitivity must be estimated with respect to the input variables.

3. Approximation of CCT using ANNs

3.1. Using the ANN to approximate the stability boundary

As discussed above, the main difficulty in solving the TSC-OPF is associated with methods to incorporate stability constraints into the optimization problem. Previous studies [19] have shown that the CCT can be approximated with high accuracy, based on the load flow data, using a polynomial function. For the purpose of CCT approximation, feed-forward ANNs have been used in many studies [20–23]. The structure of a feed-forward neural network has been thoroughly described in the literature, and is not shown here for brevity.

If the ANN can provide a nonlinear mapping between the initial load flow data and the CCTs of different faults, it can provide the gradient information, which helps increase the convergence rate of the OPF. In addition, the problem size of the TSC-OPF only slightly increases compared to the traditional OPF, with one contingency: there is one additional constraint.

3.2. Input selection

To approximate CCTs with high accuracy, it is important that parameters with a high correlation with the critical clearing time be selected as the input for the ANN. In principle, the vector of bus voltage magnitudes and angles contains the full load flow data and can thus be used as the input vector [19]. However, previous studies have shown that the prefault active power generation of the generators P_g has the most effect on the CCT of the corresponding machine. Moreover, it has been shown that P_g and CCT have a quasilinear relationship [24]. In addition to the active power output P_g, the reactive power output Q_g also influences the CCT. For a small system, [25,26] showed that very good estimation accuracy can be achieved with P_g and Q_g as the input.

4. The proposed framework for TSC-OPF

In this work, the ANNs are used to approximate CCT. Each considered contingency in the TSC-OPF is expressed using a separate ANN, as in Eq. (7). Because no new optimization variable is introduced in the proposed approach, the TSC-OPF formulation is essentially identical to the conventional OPF with additional constraints on the CCT of all considered faults. The proposed OPF formulation can be described by Eq. (1) and Eqs. (2)–(7).

4.1. Database generation and ANN training

To create the training data, the method in [19] was followed. Each operating condition is created based on the following equations:

$$P_L^i(k) = P_L^i[1 + 2\Delta P_L(0.5 - \varepsilon_{PL}(k))] \tag{8}$$

$$Q_L^i(k) = Q_L^i[1 + 2\Delta Q_L(0.5 - \varepsilon_{QL}(k))] \tag{9}$$

$$P_G^j(k) = P_G^j[1 + 2\Delta P_G(0.5 - \varepsilon_{PG}(k))] \tag{10}$$

$$U_G^j(k) = U_g^j[1 + 2\Delta U_g(0.5 - \varepsilon_{Ug}(k))], \tag{11}$$

where $P_L^i(k)$ and $Q_L^i(k)$ are the initial load demand at bus i and $P_G^j(k)$ and $U_G^j(k)$ are the active power and voltage set points at the jth bus. The operating point is indexed by k, and ε_{PL}, ε_{QL}, ε_{PG}, ε_{Ug} are independent random variables, which vary in the range of [0; 1]. The range of variation of the load flow data variables is controlled by parameters ΔP_L, ΔQ_L, ΔP_G and ΔU_g. In this work, dynamic simulations are performed using the MatDyn tool [27]. To improve the accuracy of simulations, the variable time step solver Runge-Kutta Fehlberg was used. CCT was determined by performing consecutive time-domain simulations with varying fault clearing times. The transient stability was assessed by observing the generators' relative angles with respect to the COI, up to a stop time of $t_s = 4$ s. A relative angle larger than 100° is considered unstable [2]. In this work only the relative angle at the stop time 4 s is assessed. With this approach, both first-swing and multiswing instability can be detected. For brevity, the detailed procedures of the CCT calculation are not shown here.

4.2. The transient stability constraints

After the ANN training has finished, an analytical function f_k that represents Eq. (7) is obtained. First- and second-order analytical expressions of f_k with respect to the input variables can be deduced. The OPF problem can now be augmented with additional transient stability constraints in the functional form. In addition, a multistep OPF is proposed: At each iteration, the functions f_k are linearized. The new transient stability constraints are as follows:

$$f_{0k} + \frac{\partial f_k}{\partial x}\Delta x \geq CCT_{min} \tag{12}$$

In Eq. (12), $x = [P_g, Q_g]^T$ is the input vector of f_k; f_{0k} is the estimated CCT value for contingency k and is evaluated at the current solution x^*; $CCT_{\min}$ is the minimum required CCT; and $\Delta x = x - x^*$. Eq. (12) can be rewritten as

$$\frac{\partial f_k}{\partial x}x \geq CCT_{\min} - f_{0k} + \frac{\partial f_k}{\partial x}x^* \tag{13}$$

Therefore, the final TSC-OPF formulation consists of Eq. (1), Eqs. (2)–(6), and N stability constraints in the form of Eq. (13).

After each OPF iteration, the convergence is evaluated based on the difference between the desired CCT values and the actual CCT. Another measure for convergence is the change in active power output of the generator after each iteration, i.e. $\Delta P_g = P_g(k) - P_g(k-1)$. Figure 1 summarizes the proposed framework.

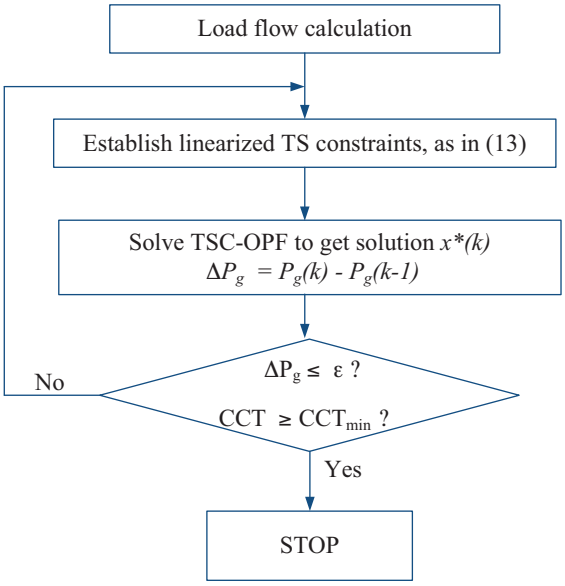

Figure 1. The proposed framework.

5. Test results

5.1. The IEEE 39 bus system

The proposed approach was first tested on the New England (IEEE 39-bus) system. A single-line diagram of this system is shown in Figure 2 [28]. The OPF problem was solved using MATPOWER [29]. In total, 2000 operating points were created. Seventy percent of this data set was used for training, and the remainder was used for testing and validation. The ANN structure (number of hidden nodes and the activation functions) was determined on a trial-and-error basis. For the New England system, the best accuracy was achieved with 35–40 nodes in the hidden layer and with the hyperbolic tangent sigmoid activation function. This result is similar to those reported in previous studies [17,21,23].

It should be noted that the transient stability of all generators should be considered in a realistic planning study. In this paper, due to limited spacing, the results of TSC-OPF are presented with 3 independent contingencies, which are three-phase faults at generators 7, 8, and 9 terminals. As discussed in Section 3.2, in this work, the combination of the generator active and reactive outputs $[P_g, Q_g]^T$ was selected as input for the ANNs.

Based on the optimal operating conditions obtained without the stability constraints, the simulation results for each of these contingencies are shown in Figure 3. The limit angle (100°) is shown is red dashed lines. The system was unstable for all considered contingencies. For generator 7, it was a multiswing instability that involved a group of generators. For generator 8, it was a multiswing instability that involved one generator only. For generator 9, it was a first-swing instability.

The stability constraints were then applied in the proposed TSC-OPF. The imposed minimum CCT for generators 7, 8, and 9 faults was 180, 180, and 110 ms, respectively. For the New England system, the solution converged at desired CCT after 2 iterations. In Figure 4, the CCTs are shown for up to 4 iterations in order to show the good convergence characteristic of the proposed algorithm.

The operating points that were obtained with OPF and TSC-OPF are shown in Table 1. It is interesting to note the active generation changes of three generators 7, 8, and 9. To mitigate the multiswing instability,

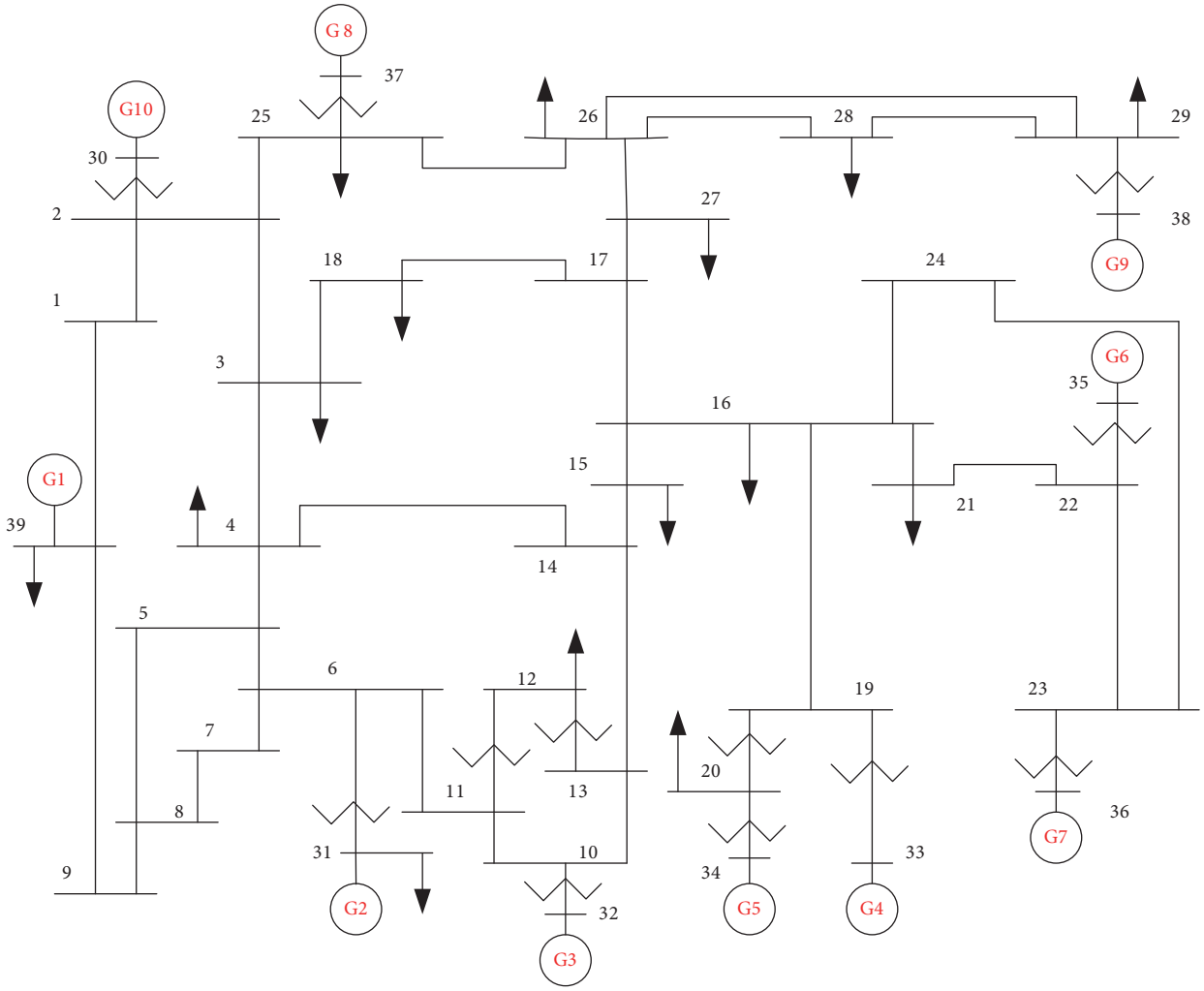

Figure 2. Single-line diagram of the New England system.

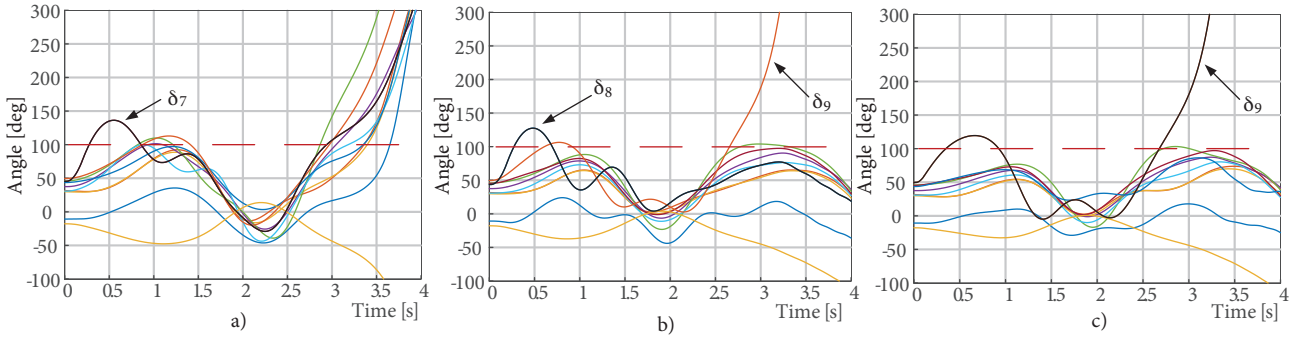

Figure 3. Angle responses of the initial OPF solution. a) 3-phase fault at G7, t_c = 180 ms; b) 3-phase fault at G8, t_c = 180 ms; c) 3-phase fault at G9, t_c = 110 ms.

generator 7 must slightly reduce its active output, whereas generator 8 does not need to change its active power at all. In fact, the reduction of active power output from the nearby generator 9 and the increase in reactive power at generator 8 are enough to stabilize the contingency.

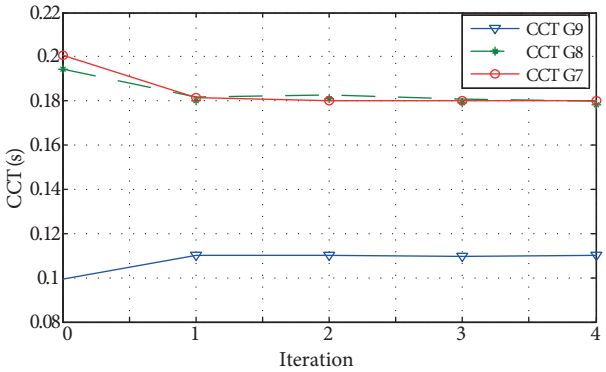

Figure 4. Convergence characteristic of the proposed TSC-OPF, New England system.

Table 1. Comparison of OPF and TSC-OPF solutions.

Machine	OPF solution			TSC-OPF solution		
	P_g (MW)	$\underline{U}_g$(pu)	Q_g (MVAr)	P_g (MW)	U_g (pu)	Q_g (MVAr)
1	274.99	1.04	140.00	274.99	1.04	140.00
2	622.07	1.03	300.00	698.11	1.00	282.24
3	617.62	1.02	263.86	698.35	0.99	218.80
4	602.16	1.01	116.64	614.19	1.01	118.60
5	558.79	1.02	157.37	499.33	1.02	167.00
6	607.02	1.06	227.95	585.08	1.06	230.28
7	615.96	1.06	71.53	610.70	1.06	75.61
8	593.97	1.03	0.00	593.97	1.03	20.26
9	912.99	1.04	53.70	822.36	1.04	27.30
10	900.13	1.01	-7.58	902.60	1.01	33.55

The angle responses of the aforementioned contingencies were now reevaluated. The results are shown in Figure 5. The system is stabilized with the TSC-OPF. It should be noted that the relative transient angle may exceed 100°, but the generators can still remain in synchronism afterward. The 100° limit is thus quite conservative; therefore this criterion is only applied at the stop time to avoid this issue.

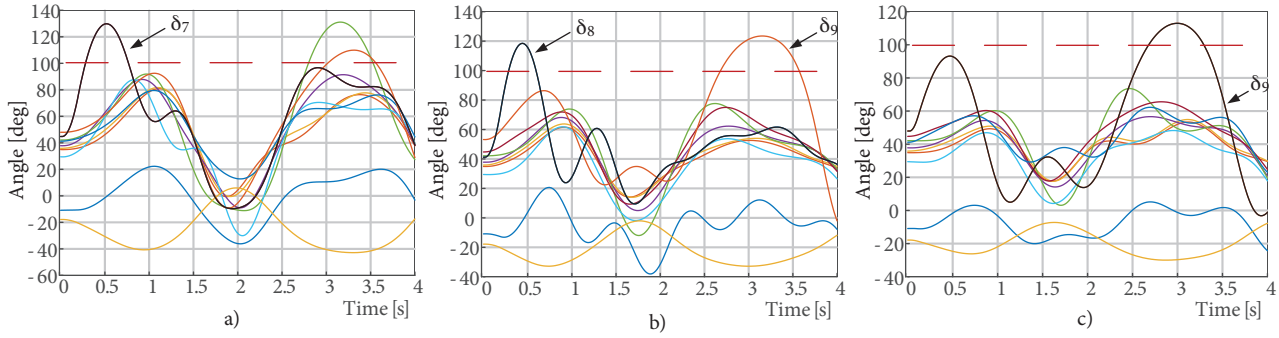

Figure 5. Angle responses of TSC-OPF solution. a) 3-phase fault at G7, t_c = 180 ms; b) 3-phase fault at G8, t_c = 180 ms; c) 3-phase fault at G9, t_c = 110 ms.

To evaluate the consistency of the proposed algorithm, the TSC-OPF was performed with 100 different initial operating points. For this test, the original cost data of the New England system were used. Table 2 shows the performance of the proposed algorithm and other algorithms for solving TSC-OPF of the New

England system. Because of the difference in the contingencies and in the generator model, an algorithm with smaller reported costs is not necessarily better than the others. The costs are shown to compare the consistency of different approaches. All algorithms shown in Table 2 have consistent performance with very small deviations. However, the proposed approach has better performance in terms of accuracy control and particularly CPU time.

Table 2. Performance comparison of different TSC-OPF algorithms.

	Proposed method	Ref [14]	Ref [13]	Ref [12]
Maximum cost ($/h)	36,349	36,368	36,413	-
Minimum cost ($/h)	36,318	36,350	36,382	-
Standard deviation	10.7 $ (<0.01%)	5.09 (<0.01%)	-	0.05%
CCT error (ms)	≤ 5	≤ 10	≤ 10	10
CPU time (s)	0.89	145	950.8	86–91

5.2. IEEE 300 bus system

The proposed TSC-OPF approach was also tested on the IEEE 300 bus system with 69 generators. The load flow and generator cost data for this system are available in MATPOWER. The dynamic data for this system were created using the IEEE AC4A excitation model and TGOV1 governors. Three contingencies were selected to evaluate the performance of the proposed algorithm: 3-phase faults at generators 6, 21, and 40. With the original load flow and generator cost data, the CCT for these contingencies are 110, 220, and 76 ms, respectively. Since the fault-clearing time of modern digital relays and circuit breakers is typically in the range of 80–100 ms, the CCT of generator 6, and especially that of generator 40, are rather small. Therefore, the CCT levels of these generators are set to 180 ms and 200 ms, respectively.

After the proposed TSC-OPF converged to the optimal solution, time-domain simulations were performed to determine the CCT of the considered contingencies. As seen in Table 3, the actual CCT for generators 6 and 40 were 183 and 204 ms, which satisfied the imposed constraints. The simulation results are not shown, due to limited space. Because generator 21 was already stable with the fault being considered, the TSC-OPF did not affect its CCT value.

Table 3. Comparison of desired values of CCT and their actual values.

Gen.	Desired CCT (ms)	Actual CCT (ms)
6	180	183
21	180	220 (nonbinding)
40	200	204

The average CPU time of the proposed TSC-OPF algorithm is 3.5 s for the IEEE 300 bus system. To solve the TSC-OPF of this system with multiple contingencies, the reported CPU time is 69.66 s in [18], 23 s in [30], and 102.6 s in [31].

6. Conclusion

This paper proposes a new framework to solve the TSC-OPF problem. In the proposed approach, CCT and its sensitivity to input variables are approximated using ANNs. Compared to sequential methods, which perform time-domain simulations during OPF calculation, and compared to the heuristic methods, the proposed method achieves faster computation time. Simulation results show that the convergence rate of the proposed approach

is notably good because of the quasilinear relationship between the generators active power and the transient stability margin. Another advantage of the proposed method compared to other heuristic methods [12–18] is that CCT performance of critical faults can be controlled more precisely, thanks to the sensitivity measures provided by the ANN. The proposed algorithm can handle several types of angle stability, including first-swing and multiswing instability, which involve one or a group of generators.

Nowadays, there is an increasing need to perform stability-constrained OPF in a near-real–time framework. For such application, the time performance of OPF calculation is critical. The proposed approach allows one to perform fast TSC-OPF calculation during operation, while the database generation and ANN training can be prepared in the day ahead planning process.

Acknowledgement

This research was funded by Vietnam National Foundation for Science and Technology Development (NAFOSTED) under grant number 102.05-2013.27.

References

[1] Kundur P, Paserba J, Ajjarapu V, Andersson G, Bose A, Canizares C, Hatziargyriou N, Hill D, Stankovic A, Taylor C et al. Definition and classification of power system stability. IEEE T Power Syst 2004; 19: 1387-1401.

[2] Gan D, Thomas RJ, Zimmerman RD. Stability-constrained optimal power flow. IEEE T Power Syst 2000; 15: 535-540.

[3] Yuan Y, Sasaki H. A solution of optimal power flow with multicontingency transient stability constraints. IEEE T Power Syst 2003; 18: 1094-1102.

[4] Zárate-miñano R, Van Cutsem T, Milano F, Conejo AJ. Securing transient stability using time-domain simulations within an optimal power flow. IEEE T Power Syst 2010; 25: 243-253.

[5] Pizano-martínez A, Fuerte-esquivel CR, Ruiz-vega D. Global transient stability-constrained optimal power flow using an OMIB reference trajectory. IEEE T Power Syst 2010; 25: 392-403.

[6] Xin H, Gan D, Huang Z, Zhuang K, Cao L. Applications of stability-constrained optimal power flow in the east china system. IEEE T Power Syst 2010; 25: 423-1433.

[7] Tu X, Dessaint LA, Nguyen-Duc H. Transient stability constrained optimal power flow using independent dynamic simulation. IET Gener Transm Dis 2013; 7: 244-253.

[8] Tu X, Dessaint LA, Kamwa I. Fast approach for transient stability constrained optimal power flow based on dynamic reduction method. IET Gener Transm Dis 2014; 8: 1293-1305.

[9] Xu Y, Dong ZY, Zhao J, Xue Y, Hill DJ. Trajectory sensitivity analysis on the equivalent one-machine-infinite-bus of multi-machine systems for preventive transient stability control. IET Gener Transm Dis 2014; 9: 276-286.

[10] Fang DZ, Xiaodong Y, Jingqiang S, Shiqiang Y, Yao Z. Optimal generation rescheduling approach for transient stability enhancement. IEEE T Power Syst 2007; 22: 386-394.

[11] Hou G, Vittal V. Determination of transient stability constrained interface real power flow limit using trajectory sensitivity approach. IEEE T Power Syst 2013; 28: 2156-2163.

[12] Cai HR, Chung CY, Wong KP. Application of differential evolution algorithm for transient stability constrained optimal power flow. IEEE T Power Syst 2008; 23: 719-728.

[13] Mo N, Zou ZY, Chan KW, Pong TYG. Transient stability constrained optimal power flow using particle swarm optimisation. IET Gener Transm Dis 2007; 1: 476-483.

[14] Wu D, Gan D, Jiang JN. An improved micro-particle swarm optimization algorithm and its application in transient stability constrained optimal power flow. Eur T Electr Power 2014; 24: 395-411.

[15] Ayan K, Kılıç U, Baraklı B. Chaotic artificial bee colony algorithm based solution of security and transient stability constrained optimal power flow. Int J Elec Power 2015; 64: 136-147.

[16] Ahmadi H, Ghasemi H, Haddadi AM. Lesani H. Two approaches to transient stability-constrained optimal power flow. Int J Elec Power 2013; 47: 181-192.

[17] Tangpatiphan K, Yokoyama A. Evolutionary programming incorporating neural network for transient stability constrained optimal power flow. In: 2008 Joint International Conference on Power System Technology and IEEE Power India Conference. New Delhi, India. pp. 1-6.

[18] Mahmoudi M, Aghamohammadi MR. A new approach for transient stability constrained opf based on neural network and genetic algorithm. In: 31th Power System Conference; 2016 (PSC2016). Tehran, Iran. pp. 1-7.

[19] Jayasekara B, Annakkage UD. Derivation of an accurate polynomial representation of the transient stability boundary. IEEE T Power Syst 2006; 21: 1856-1863.

[20] Abdallah H, Chtourou M, Guesmi T, Ouali A. Feedforward neural network-based transient stability analysis of electric power systems. Eur T Electr Power 2006; 16: 577-590.

[21] Karami A. Estimation of the critical clearing time using MLP and BRF neural networks. Int T Electr Power 2010; 20: 206-217.

[22] Moulin LS, da Silva APA, El-Sharkawi MA, Marks RJ. Support vector machines for transient stability analysis of large scale power systems. IEEE T Power Syst 2004; 19: 818-825.

[23] Karami A. Power system transient stability margin estimation using neural networks. Int J Elec Power 2011; 33: 983-991.

[24] Pizano-Martinez A, Fuerte-Esquivel CR, Ruiz-Vega D. A new practical approach to transient stability-constrained optimal power flow. IEEE T Power Syst 2011; 26: 1686-1696.

[25] Wehenkel LA. Automatic Learning Techniques in Power Systems. New York, NY, USA: Springer, 1998.

[26] Sulistiawati I, Priyadi A, Qudsi O, Soeprijanto A, Yorino N. Critical clearing time prediction within various loads for transient stability assessment by means of the extreme learning machine method. Int J Elec Power 2016; 77: 345-352.

[27] Cole S, Belmans R. MatDyn, a new MATLAB-based toolbox for power system dynamic simulation. IEEE T Power Syst 2011; 26: 1129-1136.

[28] Pai MA. Energy Function Analysis for Power System Stability. New York, NY, USA: Springer, 1989.

[29] Zimmerman RD, Murillo-Sanchez CE, Thomas RJ. Matpower: steady state operations, planning and analysis tools for power systems research and education. IEEE T Power Syst 2011; 26: 12-19.

[30] Geng G, Ajjarapu V, Jiang Q. A hybrid dynamic optimization approach for stability constrained optimal power flow. IEEE T Power Syst 2014; 29: 2138-2149.

[31] Jiang Q, Geng G. A reduced-space interior point method for transient stability constrained optimal power flow. IEEE T Power Syst 2010; 25: 1232-1240.